Geomechanics and Engineering, *Vol. 34, No. 2 (2023) 173-186*
https://doi.org/10.12989/gae.2023.34.2.173

Evaluation of the geogrid-various sustainable geomaterials interaction by direct shear tests

Bahadir Ok*, Huseyin Colakoglu and Umud Dagli

Department of Civil Engineering, Alparslan Turkes Science and Technology University, Balcalı Neighborhood, Çatalan Street No:201/1 01250 Sarıçam, Adana, Turkey

(*Received December 20, 2022, Revised May 15, 2023, Accepted May 16, 2023*)

Abstract. In order to prevent environmental pollution, initiatives to increase the sustainability of resources are supported by society. However, the performance of recycled materials does not generally match that of natural materials. This study looks into the use of geogrid to improve various types of recycled aggregates. For this purpose, five different recycled aggregates were created by recycling wastes from the construction industry. Besides, direct shear tests (DS tests) were carried out on these recycled aggregates to determine their shear strengths. Following that, a triaxial geogrid was placed in the recycled aggregates to provide reinforcement, and the DS tests were conducted on the reinforced recycled aggregates. The results of the tests were also compared to those of tests performed on natural aggregates (NA). In conclusion, it was found that the recycled aggregates have lower shear strengths than the NA. Nonetheless, when reinforced with geogrid, the shear strength of the recycled concrete aggregates (RCA) and construction and demolition wastes (CDW) exceeded that of the NA. Furthermore, the geogrid reinforcement increased the shear strength of the recycled crushed bricks (CB), though not to the level of the NA.

Keywords: direct shear test; granular soils; recycled aggregate-geogrid interaction; recycled materials; sustainability

1. Introduction

The sustainability of natural resources used in the construction industry is now a requirement due to environmental concerns and increasing costs. Natural aggregates derived from quarries are one of the most commonly consumed natural resources in the construction industry. The natural aggregates are supplied from the quarries by excavating or exploding rocks beneath the ground surface. Besides, access roads should be constructed for the transportation of natural aggregates. These processes could harm the environment since quarries are generally widespread in the natural environment. On the other hand, the increasing transportation and energy costs cause a need for alternative resources (Han and Thakur 2014, Vieira and Pereira 2015a, Saribas and Ok 2019, Akpinar and Attar 2021).

Construction activities lead to the production of debris called "construction and demolition waste" (CDW). The CDW is a heterogeneous mixture of various wastes. Concrete, brick, tile, ceramic, wood, glass, plastic, bituminous mixtures, soil, and metals could be constituents of the CDW. The concrete particles in the CDW could be separated by using some techniques. After some recycling processes, these concrete particles, known as recycled concrete aggregates (RCA), could be reused in some civil engineering applications. Also, brick particles in the CDW, known as recycled crushed bricks (CB), are considered to have the potential to be used as filling materials (Arulrajah *et al*. 2013a, Cabalar *et al*. 2016). Furthermore, the recycling percentage would be increased if the CDW could be reused without separating concrete and brick particles after some recycling processes. Accordingly, studies on the reuse of CDW have been conducted similar to studies on RCA and CB. However, many researchers found that the strengths of recycled aggregates, such as the CDW, RCA, and CB, were lower than those of natural aggregates in studies on recycled aggregates (Ok *et al*. 2020, Mehrjardi *et al.* 2020). This circumstance reduces the usage percentage of recycled aggregates. Accordingly, several researchers proposed that improving recycled aggregates would increase their use. Following this, researchers investigated the use of geosynthetics (Arulrajah *et al.* 2013b, Rahman *et al.* 2014, Santos *et al.* 2013, Vieira and Pereira 2015b) or additive materials such as cement, fly ash, alkali activator, and geopolymers to improve recycled aggregates (Arulrajah *et al.* 2016, Mohammadinia *et al.* 2019a, b, Perera *et al.* 2019, Yaghoubi *et al.* 2017, Bruschi *et al.* 2022).

A variety of test equipment has been developed to assess the strength parameters of granular soils (Rahmani and Panah 2020, Estévez-Ventosa *et al.* 2022). Many researchers accept that employing direct shear box test equipment can provide one of the most accurate and precise results (Alias *et al.* 2014, Arulrajah *et al.* 2014a, Lee *et al.* 2017, Park *et al.* 2022). However, Bareither *et al.* (2008) mentioned that the size of the shear box device affects the results when the soil includes gravel greater than 30%.

Accordingly, ASTM D 3080 standard reported that the width of the shear box should be at least ten times the maximum grain diameter, and the height should be at least six times the maximum grain diameter. Because of that, a

*Corresponding author, Ph.D.
E-mail: bahadirok@atu.edu.tr

ISSN: 2005-307X (Print), 2092-6219 (Online)

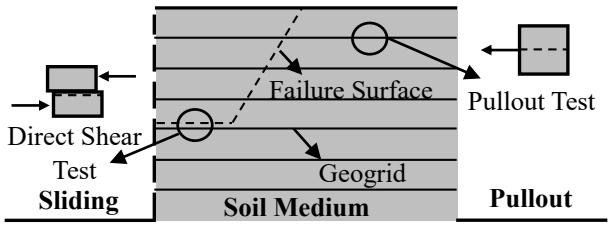

Fig. 1 The interaction mechanisms in a typical reinforced-soil retaining wall: sliding and pullout to be modeled by the direct shear and pullout tests(revised from Naeini *et al.* 2013)

direct shear test apparatus whose shear box's dimensions are larger than those of a conventional shear box (6 x 6 cm) is needed for determining the shear strength of coarse-grained soil specimens (Tu *et al.* 2022) On the other hand, to better understand soil-geogrid interaction, a variety of tests have been used, including plane strain tests (Li *et al.* 2012), torsional ring shear tests (Tan *et al.* 1998), direct shear tests (Han *et al.* 2017), and pull-out tests (Ren *et al.* 2018, Kayadelen *et al.* 2018). However, many researchers have used pull-out or direct shear tests to study the interaction behavior of the soil-geogrid interface because of their reasonable ability to capture the mechanisms found in typical reinforced soil structures (Naeini *et al.* 2013). Fig. 1 depicts the sliding and pullout interaction mechanisms that can be modeled schematically by these tests (Palmeira and Milligan 1989).

According to Athanasopoulos (1993), the pull-out test in dense sands may produce a greater apparent friction angle than the direct shear test in circumstances under low normal stress as a result of dilatation. Furthermore, Ren *et al.* (2018) reported that pull-out tests frequently result in geogrid failure due to debonding at the geogrid soil interface. According to many researchers, large-scale direct shear tests could be appropriate for determining soil-geogrid interaction characteristics (Han *et al.* 2017, Sweta. and Hussaini 2018, Safa *et al.* 2019, Stacho *et al.* 2020). The interlocking of soil grains and the geogrid could improve the shear strength of soils by providing the aggregates with lateral confinement (Giroud and Han 2004).

The interlocking between soil grains and the geogrid could change with the variation of various parameters associated with the soil and the geogrid (Abu-Farsakh and Chen 2011). Therefore, the soil-geogrid interaction should be determined for different types of soil grains. The direct shear box test has been identified as one of the most effective methods for determining soil-geogrid interaction characteristics (Han *et al.* 2017, Stacho *et al.* 2020). Arulrajah *et al.* (2013b, 2014b) conducted studies on improving recycled aggregates by conducting large-scale direct shear tests. As a result of the tests, they reported that the large-scale direct shear tests were suitable for determining the recycled aggregate-geogrid interaction. Furthermore, they mentioned that the geogrid could be used for improving recycled aggregates. Another considerable study on the recycled aggregate-geogrid interaction was conducted by using direct shear test apparatus by Vieira and Pereira (2016). However, it was not found a study on both recycled aggregates' particle strength and composition, although they were significant parameters for recycled aggregates. These aforementioned parameters would matter for recycled aggregate-geogrid interaction. Thus, studies investigating the effects of these parameters on reinforced recycled aggregates are needed.

The effect of recycled aggregates' particle strength and composition on shear strength is the main objective of this study when recycled aggregates are reinforced by geogrid.

To the best of the authors' knowledge, the novelty of this study comes from investigating recycled aggregates with different particle strengths and various compositions through direct shear tests. For this purpose, five types of different recycled aggregates, which were two types of CDW, RCA, and a type of CB, were created by recycling construction wastes. RCAs had different particle strengths. The compositions of CDWs were also different from each other. In the beginning, five different recycled aggregate specimens were prepared by making them suitable for use as a filling material by grading. Besides, a type of natural aggregate specimen (VA) from natural aggregates supplied from a quarry was prepared by grading. Subsequently, the shear strengths of prepared specimens were determined by performing direct shear tests (DS tests). Afterwards, recycled aggregates were reinforced by geogrid, positioned in them, and fixed to the shear box, and direct shear tests were conducted on the reinforced recycled aggregates. The obtained results were presented in comparison with the results of similar tests.

2. Material

2.1 The Construction and Demolition Wastes (CDW)

The construction and demolition wastes were obtained from debris containing the various construction wastes generated as a result of the demolition of old buildings in different locations. The average concrete compressive strength of the demolished buildings was 13.9 MPA. After recycling process, two types of construction and demolition waste aggregate specimens were prepared. The recycling process consisted of removing metal parts and crushing the remaining waste. Based on ASTM D 1241-07, the remaining wastes of various sizes were mixed to create a gradation suitable for use as filling material. The construction and demolition waste aggregate specimens were called the CDW-1 and the CDW-2 separately, based on the locations they were obtained.

CDWs may contain various waste materials, including concrete, brick, glass and etc. Nevertheless, CDWs may

Table 1 The percentages of the recycled aggregates in the CDWs

Component	Unit	CDW1	CDW2
Concrete, Concrete Products, Mortar	%	62	29
Aggregate, Aggregate without Binder, Aggregate with Hydraulic Binder	%	29	63
Brick, Wall Units with Calcium Silicate	%	9	8

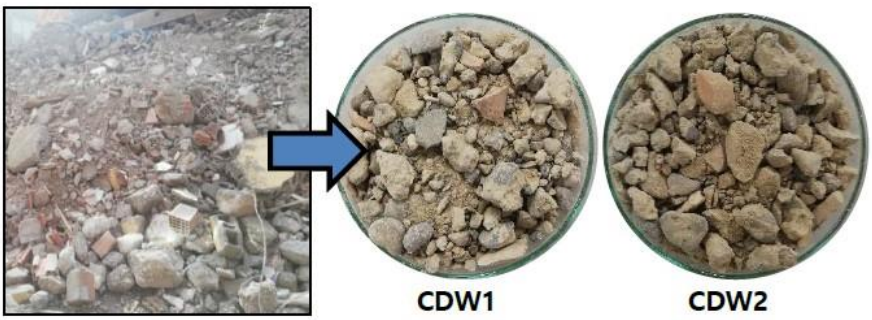

Fig. 2 The CDW1 and the CDW2, respectively

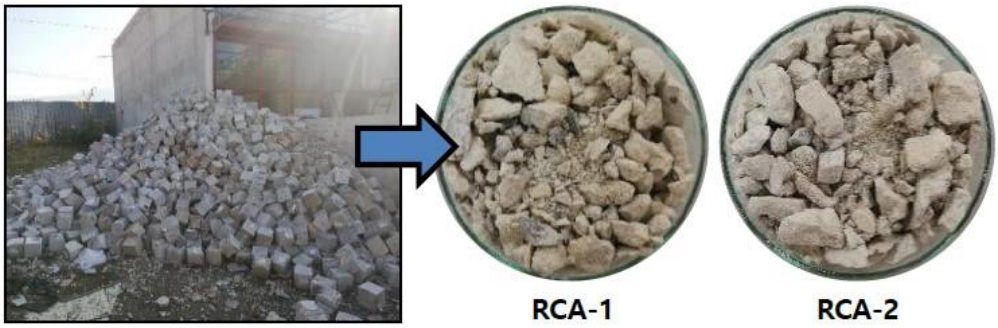

Fig. 3 The RCA-1 and the RCA-2, respectively

incorporate natural aggregates grouped as aggregate, aggregate without binder, or aggregate with a hydraulic binder (BS EN 933-11:2009). These natural aggregates are produced by crushing the debris, and their surfaces contain no binder (or mortar) (Jimenez *et al.* 2012, Cerni *et al.* 2012). The main difference between the CDW1 and the CDW2 in this study is the difference between the concrete and natural aggregate ratios they contain. Table 1 shows the material proportions in CDW1 and CDW2 (BS EN 933-11:2009). Besides, the CDW1 and the CDW2 were shown in Fig. 2.

2.2 The Recycled Concrete Aggregates (RCA)

Concrete compressive strength is one of the effective parameters that define the strength characteristics of concrete. Therefore, the compressive strength of the concrete from which the waste concrete is obtained will determine the quality of the waste concrete. Because of that, two recycled concrete aggregate specimens with different concrete compressive strengths were created from waste concrete cube specimens. For this purpose, waste concrete cube specimens whose concrete compressive strength was 25 MPa and 45 MPa were taken. Following that, the cube specimens with similar concrete compressive strength were crushed with the help of a crusher with grouping. Subsequently, the recycled concrete aggregates were mixed to have a gradation suitable for use as a filling material in filling (ASTM D 1241-07). As a result, two different RCA specimens with different strengths were produced. These RCA specimens were called RCA-1 and RCA-2 for concrete compressive strengths of 25 MPa and 45 MPa, respectively. The RCA-1 and RCA-2 are shown in Fig. 3.

2.3 The Recycled Crushed Bricks (CB)

Waste bricks are a significant component of CDW. For the scope of this study, the waste bricks that were stored in a landfill were supplied and crushed with the help of a crusher. Subsequently, the waste brick particles of different sizes were mixed to obtain the suitable gradation for a filling material. Finally, the recycled crushed brick specimens (CB) were obtained (Fig. 4).

2.4 The Natural Aggregates (NA)

One of the primary purposes of this study is to compare the performance of reinforced recycled aggregates with that of natural aggregates. Because of that, the natural aggregates were supplied from a local quarry (Altay *et al.*

Fig. 4 The CB

Fig. 5 The NA

Table 2 The geotechnical/engineering properties of specimens

Properties	CDW-1	CDW-2	CB	RCA-1	RCA-2	NA
C_u	19.17	15.91	12.00	11.53	9.32	14.40
C_c	1.23	1.05	1.15	1.26	1.22	1.65
FI (%)	10.40	9.86	26.29	14.39	14.16	9.87
LA (%)	38.6	30.0	26.9	38.7	35.9	28.3
γ_s (kN/m^3) ^{Fine}	26.58	26.54	27.27	26.23	26.17	26.60
γ_s (kN/m^3) ^{Coarse}	25.76	26.41	26.47	26.10	26.11	26.58
WA (%) ^{Fine}	11.37	11.34	20.24	10.99	8.39	3.31
WA (%) ^{Coarse}	7.69	4.53	16.71	5.77	4.94	0.83
γ_{drymax} (kN/m^3)	17.90	19.30	15.42	18.68	19.06	21.24
ω_{opt} (%)	12.00	11.25	21.15	11.86	10.65	7.3
$\gamma_{Dr=95\%}$ (kN/m^3)	18.45	20.29	14.51	18.49	19.23	21.48
$\gamma_{Dr=35\%}$ (kN/m^3)	16.59	18.50	12.92	16.66	17.47	19.78

∗ ^{Fine}: Fine particles, ^{Coarse}: Coarse particle, C_u: Coefficient of uniformity, C_c: Coefficient of curvature, FI: Flakiness index, LA: Los Angeles abrasion loss, γ_s: Particle Density, WA: Water absorption, γ_{drymax}: Maximum dry unit weight, ω_{opt}: Optimum moisture content, $\gamma_{Dr=95\%}$: Natural unit weight at D_r=95%, $\gamma_{Dr=35\%}$: Natural unit weight at D_r=35%

2021). Natural aggregates of different sizes were mixed to obtain a similar gradation to the recycled aggregate specimens prepared in this study. As a result of this process, the natural aggregate specimen (NA) was prepared (Fig. 5).

2.5 Geotechnical properties of recycled and natural aggregates

Sieve analysis, flatness index, Los Angeles abrasion, water absorption, pycnometer test, and compaction test were used to determine the geotechnical and physical properties of recycled and natural aggregates. Table 2 shows the results of the tests.

Besides, Fig. 6 shows the gradations of specimens obtained in this study and grading limits based on ASTM D 1241-07. Moreover, the soil classification of specimens was determined as GW (well-graded gravel) based on the Unified Soil Classification System.

2.6 The geogrid

As part of the study, a commercial company provided a type of triaxial geogrid used in fillings. The geogrid was made by punching polypropylene (PP) sheets. The geogrid had a triangular opening, and its nodes' thickness was greater than

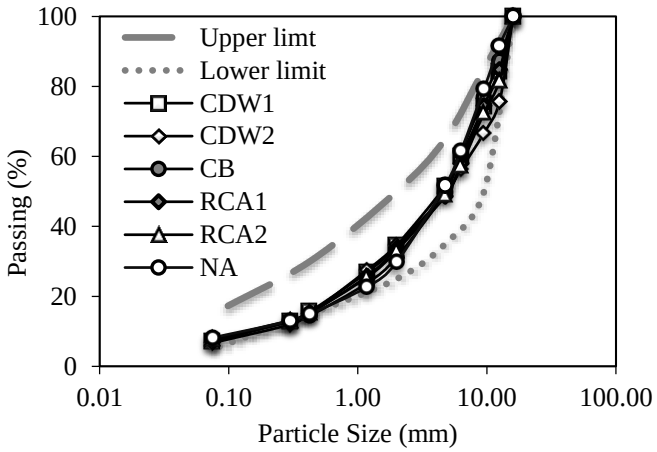

Fig. 6 Gradation curves of the specimens

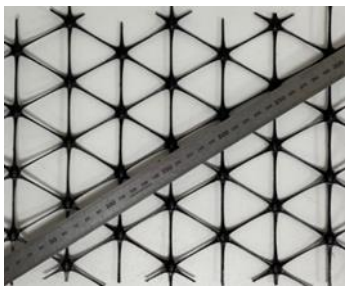

Fig. 7 The triaxal geogrid

Table 3 The characteristics of geogrid

Components	Geogrid
Raw Materials	PP
Opening Shape	Triangle
Length (mm/mm/mm)	40/40/40
Thickness (mm)	1.1
Radial Stiffness (At %0.5 deformation) (kN/m)	225

the ribs' thickness. Besides, the geogrid's aperture was 40 mm. Table 3 lists the geogrid's technical specifications. Fig. 7 shows an image of the geogrid.

3. Test procedures

In this study, the DS tests were performed on the recycled aggregate and natural aggregate specimens to determine their shear strengths. Moreover, additional DS tests were carried out on the recycled aggregate specimens reinforced by geogrid to determine the recycled aggregate-geogrid interlocking and the reinforcement effect of geogrid on the recycled aggregate specimens. The geogrid was placed beneath the shear plane to prevent sliding and sagging of the geogrid and to avoid a smooth interface at the shear plane (Arulrajah et al. 2014b). In the direct shear tests, a stiffened zone occurs beneath the shear plane. Therefore, many researchers agree that more realistic findings representing true field conditions can be achieved by positioning the geogrid just below the shear plane in the direct shear tests (McDowell *et al.* 2006, Arulrajah *et al.* 2014b). In the DS tests in this study, the geogrid's distance from the shear plane was half the maximum grain diameter ($D_{max}/2$) (Arulrajah *et al.* 2014b) Since the maximum grain diameter of the granular soil specimens obtained in this study was 15 mm (D_{max}), a larger shear box (150x150x120 mm) than that of a conventional shear box was used (ASTM D 3080) for direct shear tests. The specimens with optimum water content were compacted by placing them in the shear box in three layers to achieve the maximum dry unit weight. For compaction control, the water contents and dry unit weights of the compacted samples were determined by taking samples and weighing them before the tests. The compaction process was carried out with a vibratory hammer that gives each layer a vibration (frequency, 22–55 Hz) and an additional load (impact energy, 12 mN) to the ground for 60 seconds (ASTM 7382-08). The compacted soil specimens' relative density was between 75% and 85%. In the DS tests with geogrid, the geogrid was fixed to the bottom of the shear box and bent up from the side surface of the box. The specimen was located in the shear box layer by layer up to the geogrid's desired location. The geogrid was bent to the surface of the placed specimen. Subsequently, the specimen was located up to the top of the shear box (Fig. 8). Geogrid was fixed to both the bottom of the box and the side surface (perpendicular to the shearing direction) with a strong adhesive (epoxy) and adhesive tapes. The geogrid did not touch the two side surfaces parallel to the shearing direction due to its strong bonding and smaller size than the shear box. Also, the areas of the geogrids placed on the shear surface were equal. Besides, careful attention was paid to ensure that the number of geogrid apertures on the shear surface was the same for all tests.

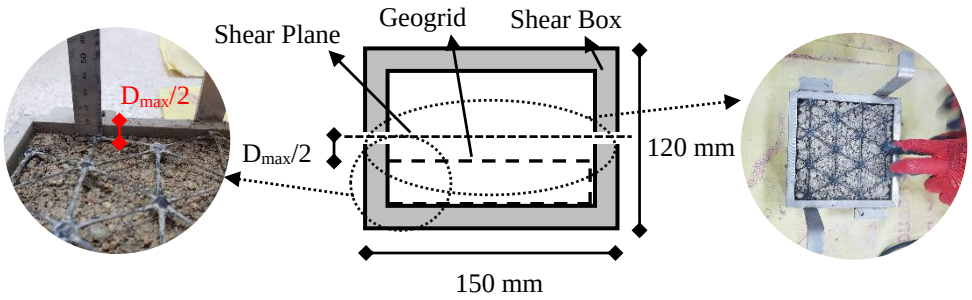

Fig. 8 The geogrid's position

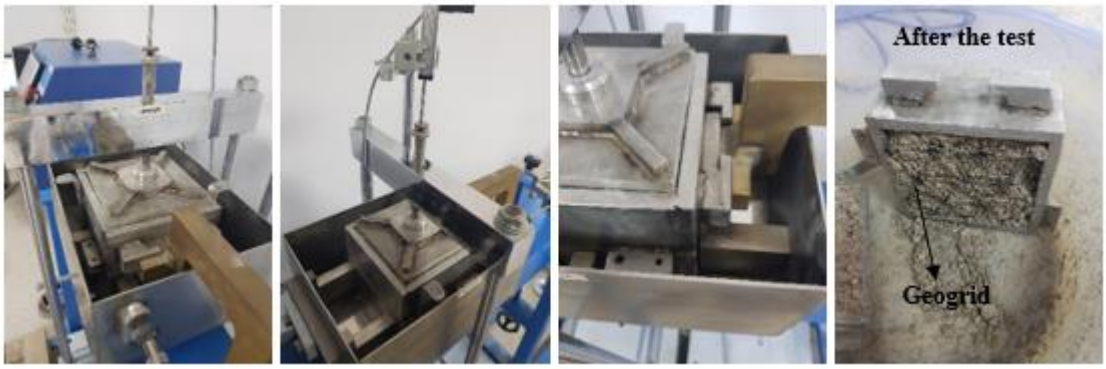

Fig. 9 The DS tests

The DS tests were performed at normal stresses of 21.8 kPa, 43.6 kPa, and 87.2 kPa with a shear deformation rate of 1 mm/min (ASTM D 3080). The bottom part of the shear box was fixed to the device while the shear force was applied to the upper part of the shear box. The shear force, vertical displacement, and horizontal displacement data were recorded by a computer with special software during the DS tests (Fig. 9). The dilatation behaviors of the specimens were investigated using vertical and horizontal strain graphs. The internal friction angles and apparent cohesions of specimens were determined with the help of the shear-normal stress graphs. Internal friction angle has a greater effect on the shear strengths of granular soils containing coarse-grained aggregates than cohesion. Therefore, the internal friction angles have been prioritized for the evaluation of the shear strength of specimens. Various researchers evaluated the shear strengths of granular soils using a similar strategy (Anubhav and Basudhar 2010, Infante *et al.* 2016, Bahaaddini 2017, Stathas *et al.* 2017, Wang *et al.* 2018).

4. Results and discussion

4.1 The shear strengths of five different recycled aggregates

The shear stress and vertical strain versus horizontal strain curves for the CDW and RCA are shown in Fig. 10. The shear stresses of the specimens increased with an increase in the normal stress. These shear stresses reached a peak value and then levelled off to become residual shear stresses. Also, the peak shear stresses of CDW-2 and RCA-2 were found to be higher than the peak shear stresses of CDW-1 and RCA-1 (Figs. 10(a) and 10(b)). Vertical strain versus horizontal strain curves, on the other hand, demonstrated that an initial vertical compression occurred until specimens could no longer compress under normal stress. Following, dilation took place (Figs. 10(c) and 10(d)). An increase in normal stress applied to the specimens resulted in higher initial compression, like in dense soil mass (Arulrajah et al. 2014b). However, increasing the normal stress caused a reduction in the expansion. The stress transferred to the shear plane is expected to increase as the normal stress increases. As a result, the specimen is under a great deal of stress, making it unable to expand easily when shearing. This phenomenon causes increasing interlocking forces. The specimens could show different failure mechanisms depending on the normal stress, such as dilatancy failure (volume expansion in dense soil) or bulging failure (volume contraction in loose soil). A similar conclusion has been reported by Mehrjardi *et al*. (2020).

Figs. 11(a) and Fig. 11(b) compare the shear strengths of the CDW, RCA, and CB specimens. Apparent cohesion was thought to have been obtained because the specimens were at their optimum water content and had well-graded gradations incorporating fine material. However, the results of the DS tests on the CDW, RCA, and CB specimens revealed that their apparent cohesion values were very close (approximately 20–22 kPa). Therefore, the comparison of specimens' shear strengths was based mostly on the internal friction angle. The internal friction angles of CDW-1 and CDW-2 specimens were determined to be 48.8 and 54.6 degrees, respectively. The percentage of aggregates without a binder (the natural

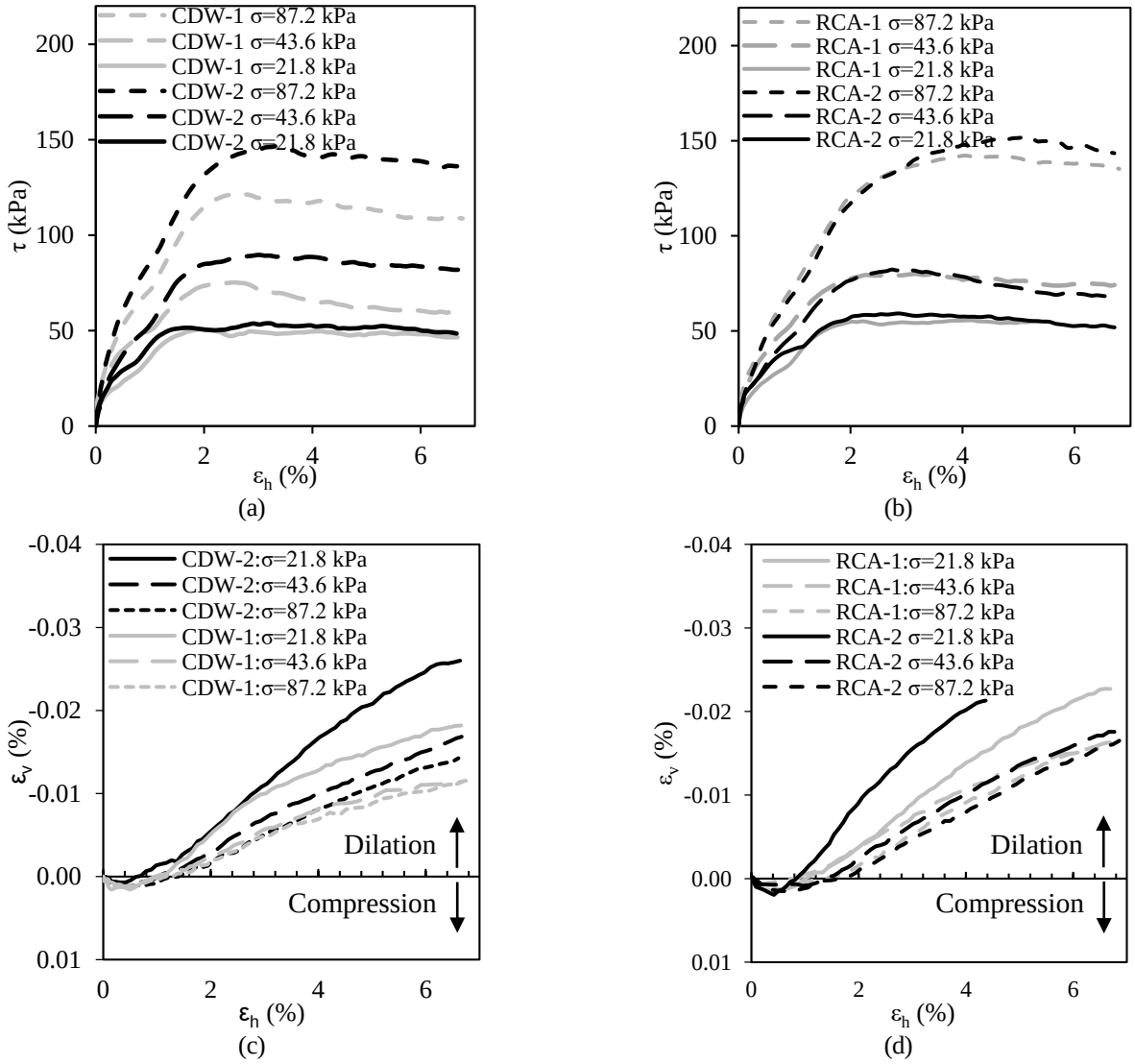

Fig. 10 The displacement behavior of the CDWs and the RCAs (a) and (b) The shear stress versus vertical strain curves of the CDWs and the RCAs (c) (d) The vertical strain versus horizontal strain curves of the CDWs and the RCAs

aggregates) in CDW-2 was approximately twice that of CDW-1. It has been considered that the difference between the compositions of the CDW-1 and CDW-2 creates a difference in their shear strengths. The strength of the natural aggregate particles in the CDW-1 and CDW-2 was greater than that of the concrete and brick particles. When the percentage of natural aggregate particles in CDW increased by 30%, the internal friction angle increased by 12% approximately. The internal friction angle of the CB specimen was determined to be 52.0 degrees. It was considered that the high flatness index and low roughness of the CB specimen's brick particles adversely affected its shear strength. In addition, the high optimum water content of the brick particles would increase the water consumption in the filling. On the other hand, it is considered that the gradation of the specimens, which was well-graded and included fine as well as coarse grains, is the fundamental reason for obtaining such cohesion and friction angle values. Another reason could be doing direct shear tests using a device with a shear box larger than that of conventional devices. Many researchers carried out direct shear tests on soils with gravel and reported cohesion and internal friction angle values close to the ones obtained in this study. Infante *et al.* (2016) reported the internal friction angle and cohesion values of the well-graded sand soil with D_{max} = 9.53 mm as 59° and 31 kPa, respectively. Arulrajah et al. (2014b) measured 57–65° friction angle and 87–95 kPa cohesion values for recycled material, with a gradation similar to the ones used in this study. Kim and Ha (2014) determined the internal friction angle of soil with D_{max} = 15.9 mm as 54°.

4.2 The reinforcement effect of geogrid on the recycled aggregates

The vertical strain versus horizontal strain curves of the CDW-1, CDW-2, RCA-1, and RCA-2 reinforced with the geogrid are shown in Fig. 12 by comparing them with their unreinforced cases. When the geogrid is placed beneath the shear plane, the geogrid interlocks with the aggregate particles,

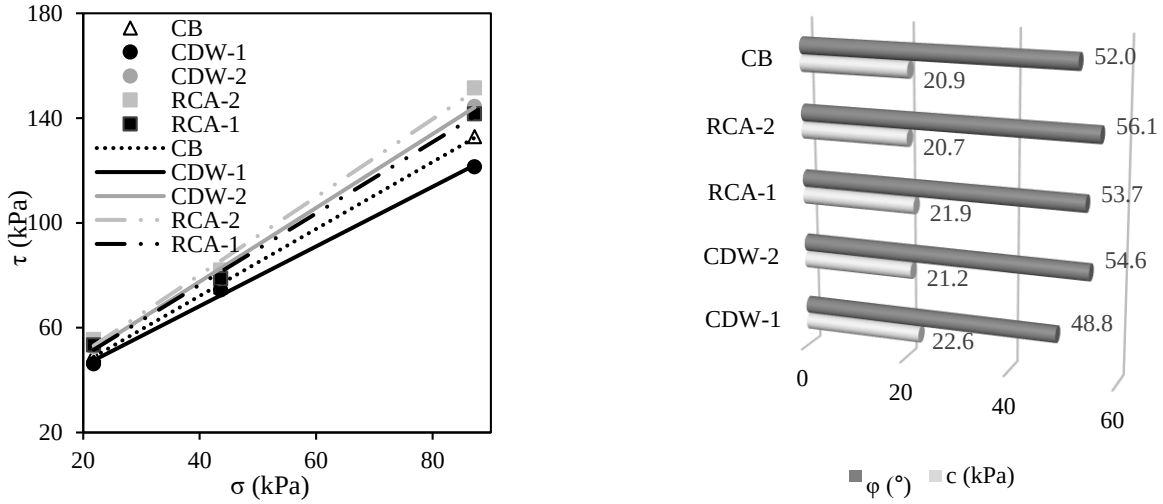

(a) (b)

Fig. 11 The shear strengths of recycled aggregate specimens

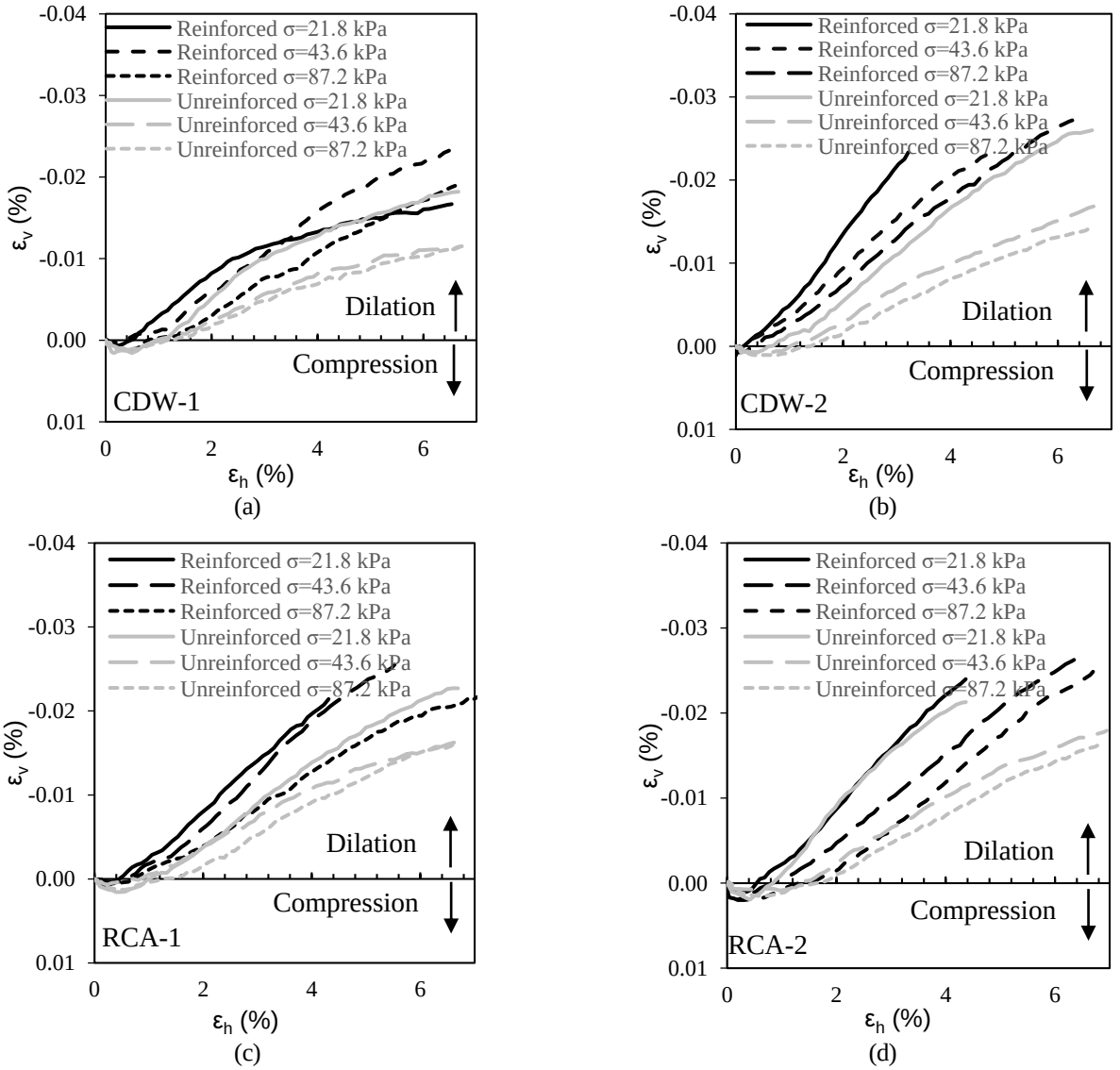

(a) (b)

(c) (d)

Fig. 12 The dilatancy behaviors of reinforced and unreinforced geomaterials (a) the CDW-1, (b) the CDW-2, (c) the RCA-1, and (d) the RCA-2

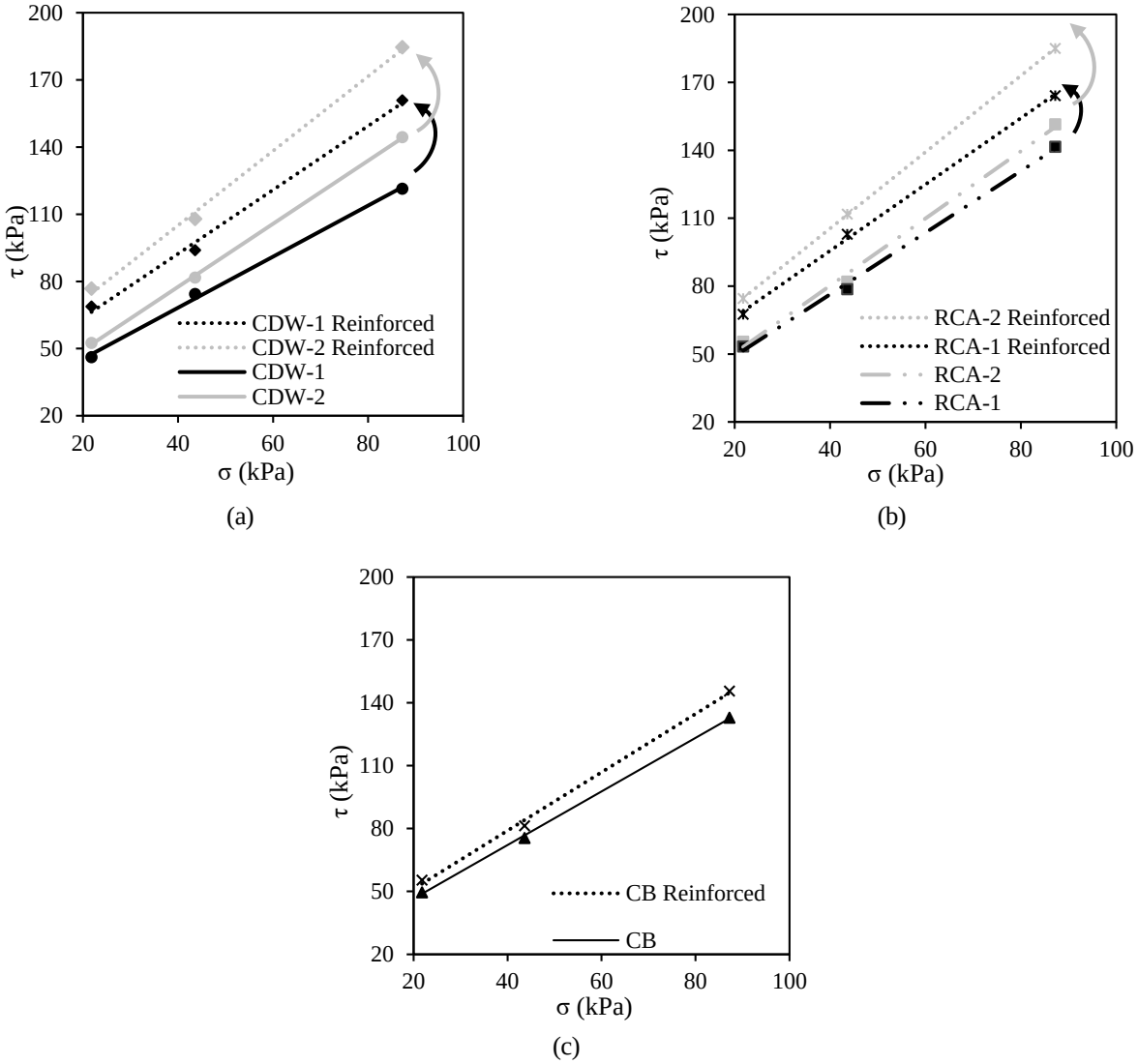

Fig. 13 The shear strength envelopes for reinforced and unreinforced recycled aggregates (a) the CDWs, (b) the RCAs and (c) the CB

forming a rigid layer at the shear plane above the geogrid (Arulrajah *et al.* 2014b). In this study, the effect of this rigid layer was also observed in the vertical strain versus horizontal strain curves. When the geogrid was placed in the specimens, the initial vertical compression values decreased while the dilatation values increased, similar to dense materials that show lower compression and higher expansion. While the initial vertical compression values were more pronounced in the tests without the geogrid (the unreinforced cases), the dilatation values were higher in the tests with the geogrid (the reinforced cases). This could imply that the interlocking of the soil grains and the geogrid creates a stiffer soil, analogous to the rigidity of dense soils compared to loose soils. Therefore, this may lead to dilatancy failure of the soil rather than bulging failure. On the other hand, as normal stress increases, stress transferred to the shear plane increases, causing increasing interlocking forces. Therefore, the specimen can expand less when shearing under high normal stress than under low normal stress. This phenomenon causes higher dilatancy under low normal stress than under high normal stress.

The shear strength envelopes of the CDW-1, CDW-2, RCA-1, RCA-2, and CB reinforced with the geogrid are shown in Fig. 13 by comparing them with their unreinforced cases. The friction angle value obtained from the DS test reinforced with the geogrid is widely called the interface friction angle rather than the internal friction angle. The interface friction angles and apparent cohesions of the CDW, RCA, and CB specimens from the tests with geogrid are shown in Fig. 14 by comparing them with their internal friction angles and cohesions. Geogrid increased the friction angle and apparent cohesion of all specimens. Hence, it is possible to state that the geogrid could be used to improve various types of recycled aggregates. The geogrid reinforcement increased the apparent cohesion values of the specimens by about 80%, excluding the CB, to a value between 35 and 38 kPa. However, the cohesion of CB only increased by 12%. The high water absorption capacity of the CB specimen's brick particles has been thought to influence its apparent cohesion. The interface friction angles of CDW-1 and CDW-2 were greater than their internal friction

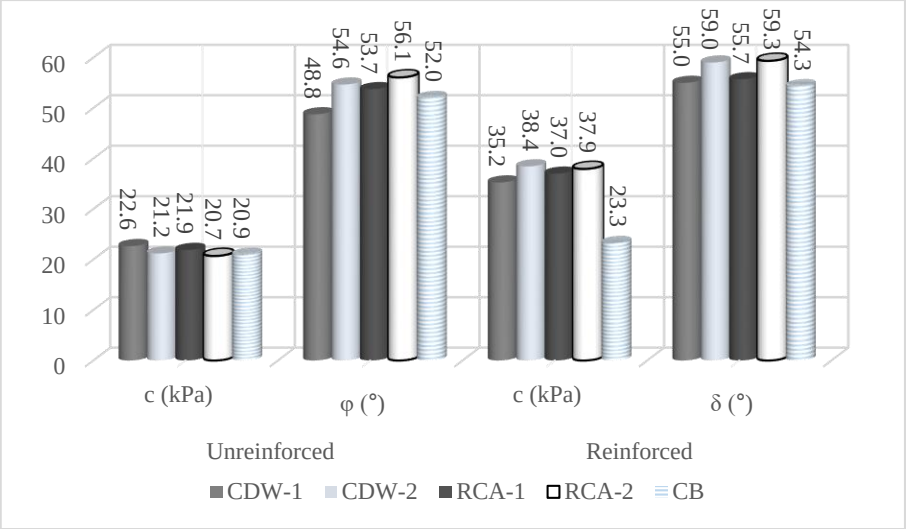

Fig. 14 The shear strength parameters for unreinforced and reinforced cases

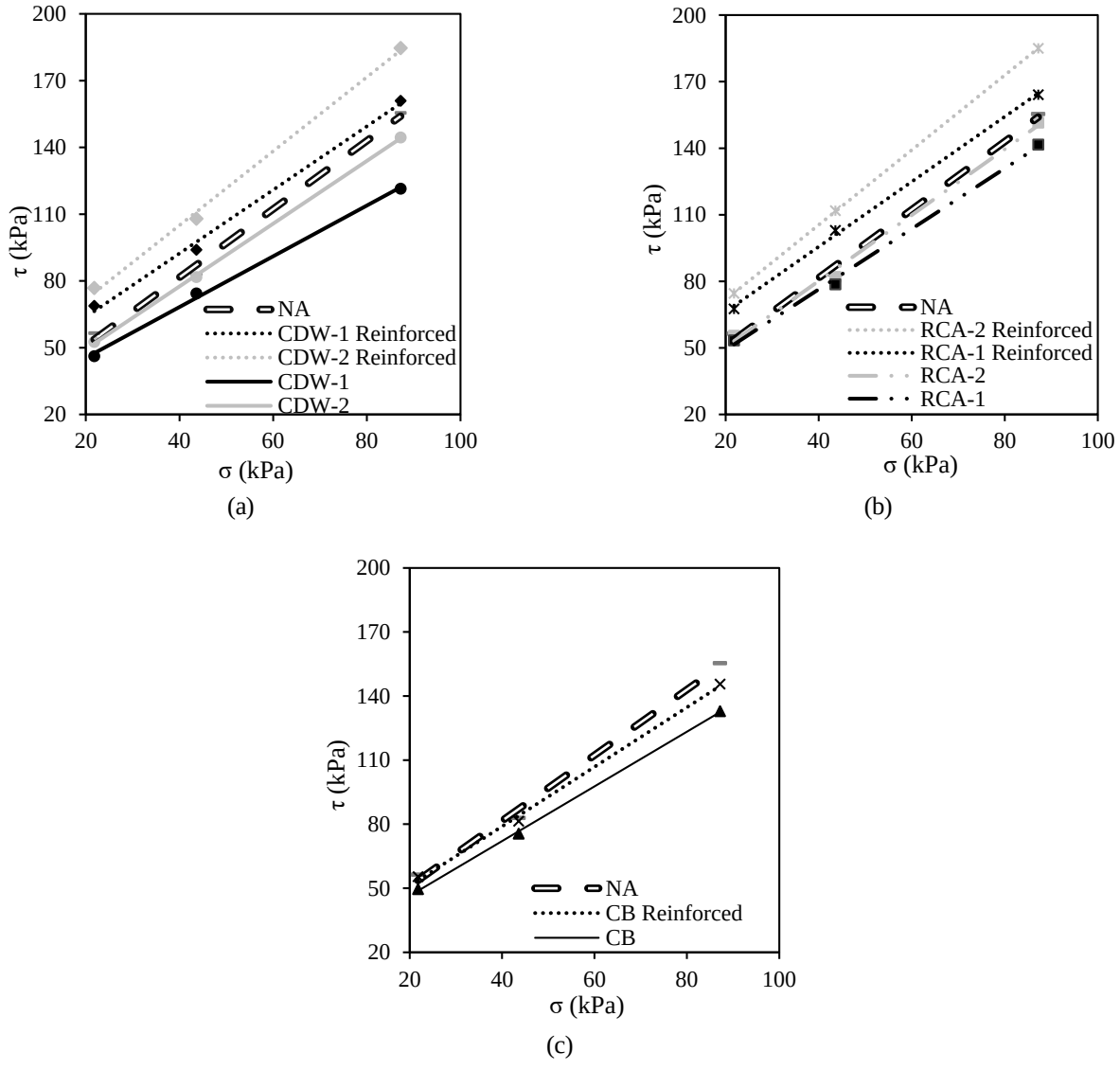

Fig. 15 The shear strength envelopes in comparison to the NA (a) the CDWs, (b) the RCAs and (c) the CB

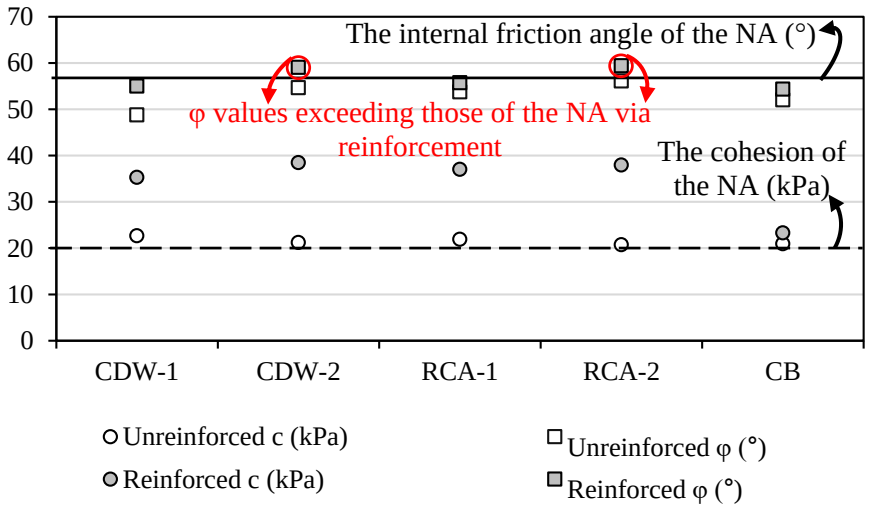

Fig. 16 The comparison of the NA's shear strength parameters with those of the recycled aggregate specimens, reinforced and unreinforced

angles by approximately 13% and 8%, respectively. The lateral confinement of CDWs' grains resulting in the interlocking between CDWs' grains and the geogrid created an increase in the friction angle of greater than about 8% (Fig. 13(a)).

The interface friction angles of RCA-1 and RCA-2 were greater than their internal friction angles by approximately 4% and 6%, respectively (Fig. 13(b)). Although the improvement of the RCAs was less than that of the CDWs, it could be said that it was acceptable (approximately 5%). The internal friction of the grains with low strength could be improved more than those with high strength. Therefore, the difference in improvement levels could be due to variations in the grain strength of RCAs and CDWs. Demir *et al*. (2013) stated that the geogrid could improve the shear strength of natural aggregates by around 10%. In this respect, it could be mentioned that the RCA and CDW specimens in this study partially behave similarly to the NA when reinforced with the geogrid.

The geogrid increased the friction angle of CB by about 4% (Fig. 13(c)). However, because their particle strengths were comparable to those of CDWs, it would have been expected that CB would be improved similarly to CDWs by geogrid. However, this phenomenon did not become reality because the recycled brick grains in the CB are flatter than those of CDWs.

4.3 Comparison with the natural aggregates

According to the DS test result, the internal friction angle of the NA specimen was determined to be 56.9 degrees. In addition, the apparent cohesion of the NA was 20.2 kPa. In Fig. 15, the shear strength of the NA specimen is compared to the shear strengths of the recycled aggregate specimens with and without the geogrid. The shear strength parameters are presented in Fig. 16 for all cases. The internal friction angle of the NA was greater than that of the recycled aggregates, while its apparent cohesion was similar. However, the difference between the internal friction angles of NA and RCA-2 was small (less than 1 degree). It was found that the friction angles of recycled aggregates such as CDW-2 and RCA-2 could become higher than those of the NA by using the geogrid. Nonetheless, the interface friction angles of the other recycled aggregates, such as the RCA-1, CDW-1, and CB, fell short of the NA's internal friction angle. However, after they were reinforced with geogrid, their friction angles approached the internal friction angle of the NA. Furthermore, it is possible to conclude that because the cohesion values of the RCA-1 and CDW-1 increased significantly after reinforcing with the geogrid, their shear strengths passed over to the shear strength of NA (Fig. 16).

The interface shear behavior between geosynthetics and aggregate can be expressed as the interface shear strength coefficient, as given below (Eq. (1)) (Arulrajah *et al.* 2014b, Liu *et al*. 2009)

$$\alpha = \frac{\tau_{reinfroced}}{\tau_{unreinforced}} \quad (1)$$

where α = interface shear strength coefficient; and τreinforced and τunreinforced = shear strength values obtained from reinforced and unreinforced DS tests, respectively. The shear strength difference between natural and recycled aggregates can be expressed as a coefficient. The interaction shear strength coefficient is obtained from the following equation (Eq. (2))

$$\beta = \frac{\tau_{natural\ aggregate}}{\tau_{recycled\ aggregate}} \quad (2)$$

where β = interaction shear strength coefficient; and τnatural aggregate and τrecycled aggregate = shear strength values obtained from DS tests with natural aggregates and recycled aggregates, respectively. Table 4 presents the interface and interaction shear strength coefficient values obtained from peak shear strength values for the normal stresses of 21.8, 43.6, and 87.2 kPa. In cases where α is greater than β, it is clear that recycled aggregates with geogrid reinforcement have a higher shear strength than natural aggregate. As a result, it has been found that the shear strengths of recycled aggregates with geogrid reinforcement, except the CB, can exceed the shear strengths of natural aggregates. It is considered that CB provides less interlocking with reinforcement than other recycled aggregates, especially due to its high flatness index.

Table 4 Comparison of interface and interaction shear strength coefficients

Specimens	Interface coefficient (α)			Interaction coefficient (β)		
	Normal stress (kPa)			Normal stress (kPa)		
	21.8	43.6	87.2	21.8	43.6	87.2
CDW-1	1.49	1.26	1.33	1.22	1.12	1.28
CDW-2	1.46	1.32	1.28	1.07	1.02	1.08
RCA-1	1.27	1.31	1.16	1.06	1.06	1.10
RCA-2	1.34	1.36	1.22	1.02	1.01	1.03
CB	1.12	1.08	1.10	1.14	1.10	1.17

5. Conclusions

In this study, five types of recycled aggregate specimens (CDW-1, CDW-2, RCA-1, RCA-2, and CB) were prepared. Also, a type of natural aggregate specimen (NA) was obtained. First, the shear strengths of recycled aggregate and natural aggregate specimens were determined by the DS tests and compared. Second, additional DS tests were performed to investigate the reinforcement of recycled aggregate specimens with geogrid. In these tests, the geogrid was positioned beneath the shear plane. The distance between the geogrid and the shear plane was half the maximum grain diameter. Some of the significant findings obtained are presented in the following items:

• The internal friction angle increases with the increase in the percentage of natural aggregates without a binder contained in the CDW. Even though the internal friction angle of the CDW-2 containing approximately 60% natural aggregate was lower than the NA by about 2 degrees, its friction angle was acceptable for filling.

• The interface friction angle of the CDW-2 reinforced with the geogrid exceeded the internal friction angle of the NA by 4%.

• If it is expected that the shear strength of the CDW will exceed that of the NA, the natural aggregate percentage in the CDW could be increased or the CDW could be reinforced by a triaxial geogrid.

• The compressive strength of the concrete from which the RCA was obtained affected its internal friction angle. The internal friction angle of the RCA-2 with concrete compressive strength of 45 MPa in this study was similar to that of natural aggregate.

• The apparent cohesions of all specimens were near each other (approximately 20–22 kPa). When the recycled aggregates, except CB, were reinforced with geogrid, the cohesion values increased by about 80%. This increased their shear strength.

• The shear strength of the CB reinforced with the geogrid didn't achieve that of the NA for all normal stresses. The CB had poorer interlocking with the geogrid than other specimens since it had a high optimum water content and flakiness index.

• The behaviors of the initial vertical compression and the dilatation of the sustainable geomaterials reinforced with the geogrid were found to be similar to those of dense materials, showing lower compression and higher dilatation.

• It is recommended that the brick percentage be low (less than 10%) and the natural aggregate percentage be high (greater than 60%) in recycled aggregate specimens that will be used as fill material. If these conditions cannot be met, it may be recommended to use geogrid reinforcement.

• The recycled aggregates can be used as fill material in the base and subbase layers of the roads, provided that they are reinforced with geogrid. Besides, the recycled aggregates can have the potential to be a fill material for the backfill of the retaining walls.

References

Abu-Farsakh, M.Y. and Chen, Q. (2011), "Evaluation of geogrid base reinforcement in flexible pavement using cyclic plate load testing", *Int. J. Pavement Eng.*, **12**(3), 275-288. https://doi.org/10.1080/10298436.2010.549565.

Akpinar, P. and Hiba Al Attar, H.A. (2021), "A case study on the viability of using increased quantities of recycled concrete aggregates in structural concrete for extending environmental conservation in North Cyprus", *Environ. Earth Sci.*, **80**, 367. https://doi.org/10.1007/s12665-021-09655-x .

Alias, R., Kasa, A. and Taha, M.R. (2014), "Particle size effect on shear strength of granular materials in direct shear test", *Int. J. Civil Archit. Struct. Constr. Eng.*, **8**(11), 1144-1147.

Altay, G., Kayadelen, C., Çanakcı, H., Bağrıaçık, B., Ok, B., and Oğuzhanoğlu, M.A (2021), "Experimental investigation of deformation behavior of geocell retaining walls", *Geomech. Eng.*, **27**(5), 419-431. https://doi.org/10.12989/gae.2021.27.5.419.

Arulrajah, A., Piratheepan, J., Disfani, M.M. and Bo, M.W. (2013a), "Geotechnical and geoenvironmental properties of recycled construction and demolition materials in pavement subbase applications", *J. Mater Civil Eng.*, **25**(8), 1077-1088. https://doi.org/10.1061/(ASCE)MT.1943-5533.0000652.

Arulrajah, A., Rahman, M.A., Piratheepan, J., Bo, M.W. and Imteaz, M.A. (2013b), "Interface shear strength testing of geogrid-reinforced construction and demolition materials", *Adv. Civil Eng. Mater.*, **2**(1), 189-200. https://doi.org/10.1520/ACEM20120055.

Arulrajah, A., Disfani, M.M., Horpibulsuk, S., Suksiripattanapong, C. and Prongmanee, N. (2014a), "Physical properties and shear strength responses of recycled construction and demolition materials in unbound pavement base/subbase applications", *Constr. Build. Mater.*, **58**, 245-257. https://doi.org/10.1016/j.conbuildmat.2014.02.025.

Arulrajah, A., Rahman, M.A., Piratheepan, J., Bo, M.W. and Imteaz, M.A. (2014b), "Evaluation of interface shear strength properties of geogrid-reinforced construction and demolition materials using a modified large-scale direct shear testing apparatus", *J. Mater. Civil Eng.*, **26**(5), 974-982. https://doi.org/10.1061/(ASCE)MT.1943-5533.0000897.

Arulrajah, A., Mohammadinia, A., Phummiphan, I., Horpibulsuk, S. and Samingthong, W. (2016), "Stabilization of recycled demolition aggregates by geopolymers comprising calcium carbide residue, fly ash and slag precursors", *Constr. Build. Mater.*, **114**, 864-873. https://doi.org/10.1016/j.conbuildmat.2016.03.150.

Athanasopoulos, G.A. (1993), "Effect of particle size on the mechanical behaviour of sand-geotextile composites", *Geotext. Geomembranes*, **12**, 255-273.

ASTM D 1241-07 (2007), Standard specification for materials for soil-aggregate subbase, base, and surface courses, ASTM International, West Conshohocken, USA.

ASTM D 3080 (2011), Standard Test Method for Direct Shear Test of Soils Under Consolidated Drained Conditions, ASTM

International, West Conshohocken, USA.

ASTM D7382 (2008), Test methods for determination of maximum dry unit weight and water content range for effective compaction of granular soils using a vibrating hammer, ASTM International, West Conshohocken, USA.

Bahaaddini, M. (2017), "Effect of boundary condition on the shear behaviour of rock joints in the direct shear test", *Rock Mech. Rock Eng.*, **50**(5), 1141-1155. https://doi.org/10.1007/s00603-016-1157-z.

Bareither, C.A., Benson, C.H. and Edil, T.B. (2008), "Comparison of shear strength of sand backfills measured in small-scale and large-scale direct shear tests", *Can. Geotech. J.*, **45**(9), 1224-1236. https://doi.org/10.1139/T08-058.

Basudhar, P.K. (2010), "Modeling of soil–woven geotextile interface behavior from direct shear test results", *Geotext. Geomembranes*, **28**(4), 403-408. https://doi.org/10.1016/j.geotexmem.2009.12.005.

British Standards Institution BS EN 933-11:2009 (2009), Tests for geometrical properties of aggregates part 11: Classification test for the constituents of coarse recycled aggregate, London, United Kingdom.

Bruschi, G.J., Secco, M.P., Sousa, L., Briga-Sá, A. and Cristelo, N. (2022), "Development of facade panels with optimised thermal performance from alkali-activated stone-cutting waste", *Environ. Earth Sci.*, **81**, 331. https://doi.org/10.1007/s12665-022-10452-3.

Cabalar, A.F., Abdulnafaa, M.D. and Karabash, Z. (2016), "Influences of various construction and demolition materials on the behavior of a clay", *Environ. Earth Sci.*, **75**, 841. https://doi.org/10.1007/s12665-016-5631-4.

Cerni, G., Cardone, F. and Bocci, M. (2012), "Permanent deformation behaviour of unbound recycled mixtures", *Constr. Build. Mater.*, **37**, 573-580. http://dx.doi.org/10.1016/j.conbuildmat.2012.07.062.

Demir, A., Laman, M., Yildiz, A. and Ornek, M., (2013), "Large scale field tests on geogrid-reinforced granular fill underlain by clay soil", *Geotext. Geomembranes*, **38**, 1-15. https://doi.org/10.1016/j.geotexmem.2012.05.007.

Estévez-Ventosa, X., Castro-Filgueira, U., González-Fernández, M,A., García-Bastante, F., Mas-Ivars, D. and Alejano, L.R. (2022), "Scale effects on triaxial peak and residual strength of granite and preliminary PFC3D models", *Geomech. Eng.*, **31**(5), 461-476. https://doi.org/10.12989/gae.2022.31.5.461.

Giroud, J.P. and Han, J. (2004), "Design Method for geogrid-reinforced unpaved roads. I. development of design method", *J. Geotech. Geoenviron. Eng.*, **130**(8), 775-786. https://doi.org/10.1061/(ASCE)1090-0241(2004)130:8(775).

Han, J. and Thakur, J.K. (2014), "Sustainable roadway construction using recycled aggregates with geosynthetics", *Sustainable Cities and Society*, **14**, 342-350. http://dx.doi.org/10.1016/j.scs.2013.11.011.

Han, B., Ling, J., Shu, X., Gong, H. and Huang, B. (2017), "Laboratory investigation of particle size effects on the shear behavior of aggregate-geogrid interface", *Constr. Build. Mater.*, **158**, 1015-1025. https://doi.org/10.1016/j.conbuildmat.2017.10.045.

Infante, D.J.U., Martinez, G.M.A., Arrua, P.A. and Eberhardt, M. (2016), "Shear strength behavior of different geosynthetic reinforced soil structure from direct shear test", *Int. J. Geosynth. Ground Eng.*, **2**(17), 1-16. https://doi.org/10.1007/s40891-016-0058-2.

Jimenez, J.R., Ayuso, J., Agrela, F., López, M. and Galvín, A.P. (2012), "Utilisation of unbound recycled aggregates from selected CDW in unpaved rural roads", *Resour. Conserv. Recy.*, **58**, 88-97. https://doi.org/10.1016/j.resconrec.2011.10.012.

Kayadelen, C., Onal, T.O. and Altay, G. (2018), "Experimental study on pull-out response of geogrid embedded in sand", *Measurement*, **17**, 390-396. https://doi.org/10.1016/j.measurement.2017.12.024.

Kim, D. and Ha, S. (2014), "Effects of particle size on the shear behavior of coarse grained soils reinforced with geogrid", *Materials*, **7**, 963-979. https://doi.org/10.3390/ma7020963.

Lee, S., Chang I., Chung, M., Kim, Y. and Kee, J. (2017), "Geotechnical shear behavior of Xanthan Gum biopolymer treated sand from direct shear testing", *Geomech. Eng.*, **12**(5), 831-847. https://doi.org/10.12989/gae.2017.12.5.831.

Li, F., Peng, F., Tan, Y., Kongkitkul, W. and Siddiquee, M. (2012), "FE simulation of viscous behavior of geogrid-reinforced sand under laboratory-scale plane strain-compression testing", *Geotext. Geomembranes*, **31**, 72-80. https://doi.org/10.1016/j.geotexmem.2011.09.005.

Liu, C.N., Ho, Y.H. and Huang, J.W. (2009), "Large scale direct shear tests of soil/pet-yarn geogrid interfaces", *Geotext. Geomembranes*, **27**(1), 19–30. https://doi.org/10.1061/(ASCE)GT.1943-5606.0000150.

McDowell, G.R., Harireche, O., Konietzky, H., Brown, S.F. and Thom, N.H. (2006) "Discrete element modelling of geogrid-reinforced aggregates", *Proceedings of the Institution of Civil Engineers-Geotechnical Engineering*, **159**(1), 35-48. https://doi.org/10.1680/geng.2006.159.1.35

Mehrjardi, G.T., Azizi, A., Haji-Azizi, A. and Asdollafardi, G. (2020), "Evaluating and Improving the Construction and Demolition Waste Technical Properties to Use in Road Construction", *Transport. Geotech.*, **23**, 100349. https://doi.org/10.1016/j.trgeo.2020.100349.

Mohammadinia, A., Arulrajah, A., Horpibulsuk, S. and Shourijeh, P.T. (2019a), "Impact of potassium cations on the light chemical stabilization of construction and demolition wastes", *Constr. Build. Mater.*, **203**, 69-74. https://doi.org/10.1016/j.conbuildmat.2019.01.083.

Mohammadinia, A., Arulrajah, A., Phummiphan, I., Horpibulsuk, S. and Mirzababaei, M. (2019b), "Flexural fatigue strength of demolition aggregates stabilized with alkali-activated calcium carbide residue", *Constr. Build. Mater.*, **199**, 115-23. https://doi.org/10.1016/j.conbuildmat.2018.12.031

Naeini, S.A., Khalaj, M. and Izadi, E. (2013), "Interfacial shear strength of silty sand–geogrid composite", *Proceedings of the Institution of Civil Engineers - Geotechnical Engineering*, **166**(1), 67-75. https://doi.org/10.1680/geng.10.00118.

Ok, B., Sarici, T., Talaslioglu, T. and Yildiz, A. (2020), "Geotechnical properties of recycled construction and demolition materials for filling applications", *Transport. Geotech.*, **24**, 100380. https://doi.org/10.1016/j.trgeo.2020.100380.

Palmeira, E.M. and Milligan, G.W.E. (1989), "Scale effects in direct shear tests on sand", *Proceedings of the 12 International Conference on Soil Mechanics and Foundation Engineering*, Rio de Janeiro, Brazil, August.

Park, S., Hwang C., Choi, H., Son, Y. and Ko, T.Y. (2022), "Experimental study for application of the punch shear test to estimate adfreezing strength of frozen soil-structure interface", *Geomech. Eng.*, **29**(3), 281-290. https://doi.org/10.12989/gae.2022.29.3.281.

Perera, S., Arulrajah, A., Wong, Y.C., Horpibulsuk, S. and Maghool, F. (2019), "Utilizing recycled PET blends with demolition wastes as construction materials", *Constr. Build. Mater.*, **221**, 200-209. https://doi.org/10.1016/j.conbuildmat.2019.06.047.

Rahmani, H. and Panah, A.K. (2020), "Effect of particle size and saturation conditions on the breakage factor of weak rockfill materials under one-dimensional compression testing", *Geomech. Eng.*, **21**(4), 315-326. https://doi.org/10.12989/gae.2020.21.4.315.

Rahman, M.A., Arulrajah, A., Piratheepan, J., Bo, M.W. and Imteaz, M.A. (2014), "Resilient modulus and permanent

deformation responses of geogrid-reinforced construction and demolition materials", *J. Mater. Civil Eng.*, **26**(3), 512-519. https://doi.org/10.1061/(ASCE)MT.1943-5533.0000824.

Ren, F., Wang, G. and Ye, B. (2018), "An analytical analysis of the pullout behaviour of reinforcements of MSE structures", *Geomech. Eng.*, **14**(3), 233-240. https://doi.org/10.12989/gae.2018.14.3.233.

Vieira, C.S. and Pereira, P.M. (2015a), "Use of recycled construction and demolition materials in geotechnical applications: a review", *Resour. Conserv. Recy.*, **103**, 192-204. https://doi.org/10.1016/j.resconrec.2015.07.023.

Vieira, C.S. and Pereira, P.M. (2015b), "Damage induced by recycled construction and demolition wastes on the short-term tensile behaviour of two geosynthetics", *Transport. Geotech.*, **4**, 64-75. https://doi.org/10.1016/j.trgeo.2015.07.002.

Vieira, C.S. and Pereira, P.M. (2016), "Interface shear properties of geosynthetics and construction and demolition waste from large-scale direct shear tests", *Geosynth. Int.*, **23**(1), 62-70. https://doi.org/10.1680/jgein.15.00030

Safa, M, Maleka, A., Arjomand, M., Khorami, M. and Shariati, M. (2019)," Strain rate effects on soil-geosynthetic interaction in fine-grained soil", *Geomech. Eng.*, **19**(6), 533-542. https://doi.org/10.12989/gae.2019.19.6.533.

Santos, E.C.G., Palmeira, E.M. and Bathurst, R.J. (2013), "Behaviour of a geogrid reinforced wall built with recycled construction and demolition waste backfill on a collapsible foundation", *Geotext. Geomembranes*, **39**, 9-19. http://dx.doi.org/10.1016/j.geotexmem.2013.07.002

Saribas, I. and Ok, B. (2020), "Seismic performance of recycled aggregate–filled cantilever reinforced concrete retaining walls", *Adv. Mech. Eng.*, **11**(4), 1-11. https://doi.org/10.1177/1468794106065007.

Stacho, J., Sulovska, M. and Slavik, I. (2020), "Determining the shear strength properties of a soil-geogrid interface using a large-scale direct shear test apparatus", *Periodica Polytechnica Civil Eng.*, **64**(4), 989-998. https://doi.org/10.3311/PPci.15766.

Stathas, D., Wang, J.P. and Ling, H.I. (2017), "Model geogrids and 3D printing", *Geotext. Geomembranes*, **45**(6), 688-696. https://doi.org/10.1016/j.geotexmem.2017.07.006.

Sweta, K. and Hussaini, S.K.K. (2018), "Effect of shearing rate on the behavior of geogrid-reinforced railroad ballast under direct shear conditions", *Geotext. Geomembranes*, **46**, 251-256. https://doi.org/10.1016/j.geotexmem.2017.12.001.

Tan, S.A., Chew, S.H. and Wong, W.K. (1998), "Sand–geotextile interface shear strength by torsional ring shear tests", *Geotext. Geomembranes*, **16**(3), 161-174. https://doi.org/10.1016/S0266-1144(98)00007-7.

Tu, Y., Wang, X., Lan, Y., Wang, J. and Liao, Q. (2022), "Mechanical properties and failure mechanism of gravelly soils in large scale direct shear test using DEM", *Geomech. Eng.*, **30**(1), 27-44. https://doi.org/10.12989/gae.2022.30.1.027.

Wang, J., Guo, J., Bai, J. and Wu, X. (2018), "Shear strength of sandstone–mudstone particle mixture from direct shear test", *Environ. Earth Sci.*, **77**, 442. https://doi.org/10.1007/s12665-018-7622-0.

Yaghoubi, E., Arulrajah, A., Wong, Y.C. and Horpibulsuk, S. (2017), "Stiffness properties of recycled concrete aggregate with polyethylene plastic granules in unbound pavement applications", *J. Mater. Civil Eng.*, **29**(4). https://doi.org/10.1061/(ASCE)MT.1943-5533.0001821.